Development of a Wall Climbing Robotic Ground Penetrating Radar System for Inspection of Vertical Concrete Structures

Md Omar Faruq Howlader, Tariq Pervez Sattar, Sandra Dudley

Abstract**—**This paper describes the design process of a 200 MHz Ground Penetrating Radar (GPR) and a battery powered concrete vertical concrete surface climbing mobile robot. The key design feature is a miniaturized 200 MHz dipole antenna using additional radiating arms and procedure records a reduction of 40% in length compared to a conventional antenna. The antenna set is mounted in front of the robot using a servo mechanism for folding and unfolding purposes. The robot's adhesion mechanism to climb the reinforced concrete wall is based on neodymium permanent magnets arranged in a unique combination to concentrate and maximize the magnetic flux to provide sufficient adhesion force for GPR installation. The experiments demonstrated the robot's capability of climbing reinforced concrete wall carrying the attached prototype GPR system and perform floor-to-wall transition and vice versa. The developed GPR's performance is validated by its capability of detecting and localizing an aluminium sheet and a reinforcement bar (rebar) of 12 mm diameter buried under a test rig built of wood to mimic the concrete structure environment. The present robotic GPR system proves the concept of feasibility of undertaking inspection procedure on large concrete structures in hazardous environments that may not be accessible to human inspectors.

Keywords**—**Climbing robot, dipole antenna, Ground Penetrating Radar (GPR), mobile robots, robotic GPR.

I. Introduction

GROUND Penetrating Radar (GPR) is a Non-Destructive Testing (NDT) method that can be used to remotely sense and map objects that are buried in the ground. The capability of GPR's non-invasive technique to identify and classify subsurface features have been implemented in application fields such as oil and gas exploration, buried pipeline localization [1], locating potential buried hazards such as mine shafts and voids in the mining industry [2], [3], investigating glaciers structure and formation [4], investigating geological sites [5]. GPR applications are is making its way within the sector of civil engineering and construction industries because of the increasing need of non-destructive detection of buried objects in building materials. Subsequently, in the construction industry, GPR has been used for non- destructive damage assessment and also in recent years to quality assessment [6], mapping reinforcement bar locations, air voids and material properties of concrete [7], locating buried pipes and conduit installations [8], inspecting the integrity of road and pavement subsurface layers and bridge decks [9], [10] etc.

The operation of GPR is based on radiating electromagnetic waves into a medium and examining the reflected signal from the subsurface objects for material properties and depth information. There are mainly two categories of GPR modes: (1) Time-of-Flight (ToF) based surveying and (2) borehole surveying. The transmitter and receiver antennas are located on the surface of the earth in the ToF based system and the mapping is done based on changes in electrical properties of the subsurface layers while, in case of borehole surveying, one or both antennas are located in boreholes, and topographical subsurface properties are estimated [11]. The performance of GPR is dictated by the frequency and bandwidth required to detect the desired target in the lossy and inhomogeneous medium. Moreover, the operation frequency band is dependent on the wave propagation losses, antenna size, and size of the buried objects [12].

Although GPR can provide accurate subsurface mapping for NDT evaluations, inspection of vertical reinforced concrete structures is challenging to gain access to test sites at a high altitude as shown in Fig. 1 that shows manual NDT of a 92 m tall concrete cooling tower using GPR by an operator [13]. Here scaffolding is used to gain access. Moreover, there is an unavailability of an efficient and cost effective survey technique as all commercially available GPR systems such as StructureScan and UtilityScan from GSSI, GroundExplorer from Mala shown in Fig. 2 can cost up to tens of thousands of pounds. Also, specially trained operators are needed for on-field radar data interpretation.

Fig. 1 Manual GPR based NDT on a concrete tower [13]

Md Omar Faruq Howlader is with the School of Engineering, London South Bank University, London, United Kingdom (e-mail: howladem@lsbu.ac.uk).

(a)

(b)

Fig. 2 (a) Commercial StructureScan and GroundExplorer GPR; (b) GPR scanning of archaeological site using low frequency 100 MHz GPR systems

In this paper, a concrete wall climbing robot with on-board 200 MHz GPR is presented. The key deliverable of this project is a working prototype to demonstrate proof of concept. To realize this concept, a technique of adding extra radiating arms has been applied to a conventional 200 MHz dipole antenna to minimize its length by 40%. A low frequency system is chosen for a low-cost system development that is possible to build using off-the-shelve components without sophisticated surface mount circuit designing equipment. Moreover, low amplitude of the transmitting pulse reduces the radar's penetration capability to maximum of 50 mm and makes the GPR suitable to be implemented in concrete structure environment where reinforcements are located at 24 - 40 mm depth [13]. The design is validated by experimenting the mobile robot's climbing performance with the attached GPR system and its ability to detect specific buried targets. The paper consists of the following sections: Section II gives an overview of the existing robotic GPR inspection systems. Section III describes the proposed system design of miniaturized dipole antenna and design parameters of the robot's adhesion module using Finite Element Analysis (FEA) software. Section IV presents the assembly procedure of the hardware systems, the climbing capability of the robot and the GPR's performance. Finally, the paper concludes with a brief summary and recommendation in Section V.

II. Robotic GPR Inspection Systems

The use of subsurface sensor as a sensing modality has received very little attention in robotics compared to other sensory systems such as thermal imaging, ultrasound or x-ray. As a result, there have been quite a lot of work in manual subsurface data gathering and interpretation compared to automated systems. Most of the work found in the literature about robotic subsurface imaging using GPR is mainly used for geological explorations and landmine detections. For example, the bridge deck assessment robot by [14] is a system capable of recognizing any harm to the bridge deck early without shutting down the traffic, highlighting zones which require fast repairs and henceforth constraining the effect on Washington's traffic. Fig. 3 shows the system in operation using 2GHz GPR with a total of 32 antennas.

Robotic field testing of underground pipe inspection using a combination of camera, LIDAR and GPR is reported in [15]. The system called 'SewerVUE' in Fig. 4 (a) can penetrate 60 cm – 2 m using antenna frequency ranging from 500 MHz – 2.6 GHz. It has two GPRs attached to its two arms which enables the robot to capture defect information along the 9 o'clock to 3 o'clock positions of a pipe section. Yeti robot [16] shown in Fig. 4 (b) is a system to automatically classify GPR images of the crevasses on ice sheet. It implements hidden Markov model based machine learning algorithm for real-time analysis and detection. Yeti uses 400 MHz antenna and tows the GPR along the polar ice surface and reports rough estimates of the crevasses location, depth, width, and snow bridge thickness.

Fig. 3 Operation of GPR bridge deck assessment robot [14]

While the robotic GPR inspection system has definitely gained some improvements in geological applications, GPR based inspection of vertical concrete structure is still facing challenges of hazardous environments such as nuclear industrial environments, working at high altitude, and limited maneuverability [17]. Therefore, the vertical concrete wall climbing robot presented in this paper can prove the concept of effective robotic GPR system for concrete structures.

Fig. 4 Sewervue [15] and Yeti Robot [16] in operation

III. System Design

Fig. 5 shows a block diagram of the GPR system that consists of a pulse generator, transmitting and receiving antenna and a digitizer for data visualization. The pulse generator generates a train of monocycle pulses which are radiated by the transmit antenna into the concrete. The radiating signals are reflected off the concrete surface and subsurface objects such as reinforcement bars due to changes of their dielectric properties. They are captured by the receive antenna and visualized by the oscilloscope. A Gaussian pulse of 5 ns width which corresponds to 200 MHz of centre frequency is chosen which facilitates easier configuration of other framework components such as antennas. A low frequency system has been chosen to develop a low cost system built from off-the-shelve components.

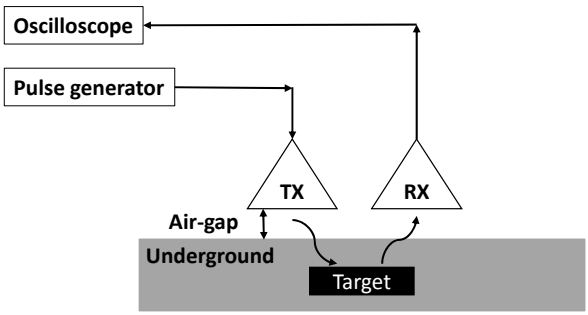

Fig. 5 Block diagram of the GPR

A. Antenna Miniaturization

For GPR applications, the dipole antennas are usually fabricated using two triangular metallic sheets as its two radiating arms and are chosen for this work as they are easy to fabricate on a variety of substrates because of planer surface structure. In theory, the length of a dipole antenna is half of its most minimal working wavelength, λ. The half-wavelength size of 670 cm at 200MHz is not feasible for better portability, it is extremely desirable to scale down the dipole antenna length so as to scale down the entire framework size.

In order to miniaturize a 200 MHz dipole antenna, dipole antenna with multiple radiating arms that is shown in Fig. 6 is proposed. The antenna is printed on a 1.6 mm thick FR4 substrate using 17 µm thick copper layer and is centre fed by 50 Ω coaxial cable. A parametric study of the distance between the primary dipole arm and extra radiating arm, *g* and length of the secondary arms, *l* is carried out using FEKO electromagnetic simulation software to establish an optimum dimension for the dipole length reduction.

Firstly, the additional antenna arm's length, l is varied from 150 mm to 50 mm, *g* = 20 mm and the reflection coefficient, S11 plot is recorded. Fig. 7 (a) shows the S11 values for various lengths. It is noticeable that, reduction in additional arm's length results in higher resonance frequency and lower S11values. The length of additional arms is selected to be 100 mm for an acceptable antenna performance, which offers -17.69 dB of S11 value at 199 MHz resonant frequency.

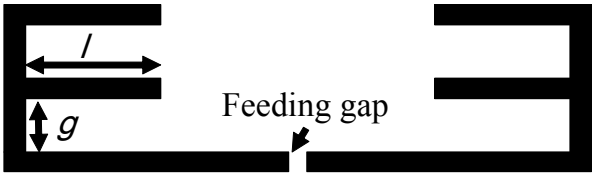

Fig. 6 Proposed miniature 200 MHz dipole antenna

To investigate the effect of the gap between the dipole arm and the extra radiating arms, g, g values are varied from 10mm to 50 mm while the additional arm's length is kept constant to 100mm. According to S11 graph given in Fig. 7 (b), at g = 10 mm, the antenna resonates at 164 MHz with S11 of -11.84 dB. Even though this results in a significant amount of dipole length reduction, for impedance and centre frequency matching, *g* = 20 mm is selected as optimum which resonates at 199 MHz with -17.84 dB of S11 and 9 MHz bandwidth. As the gap is increased to 50 mm gradually, the resonance frequency increases to 215 MHz.

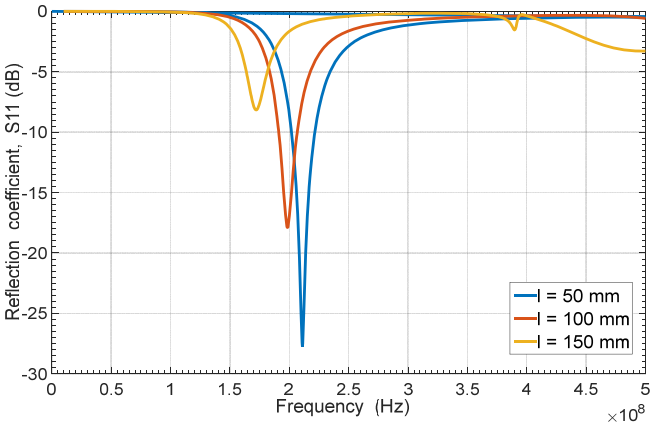

(a)

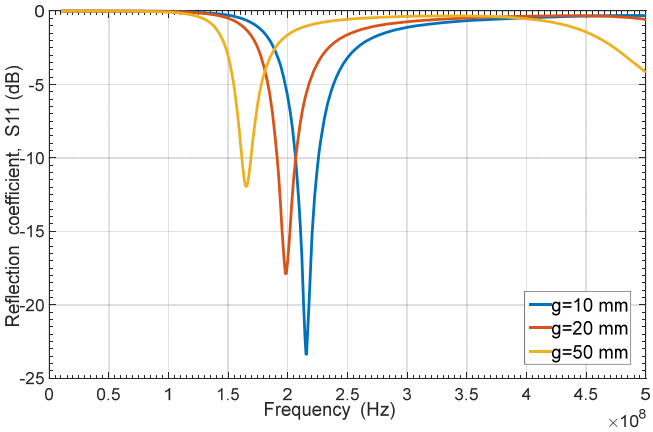

(b)

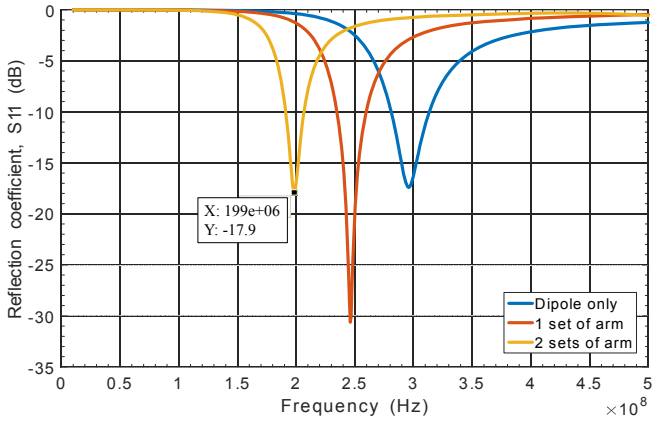

(c)

Fig. 7 Reflection coefficient, S11 values for: (a) different lengths extra of radiating arm, *l;* (b) different gap between the arms, *g;* (c) number of extra radiating arm sets

Lastly, the effect of implementing multiple sets of additional arm in antenna performance is carried out using previously selected optimum values of g = 20 mm and l = 100 mm. Without any additional arms, the antenna is a pure dipole that radiates at 300 MHz, while one set of extra radiating arm brings the resonance down to 246 MHz and two sets of arm bring the resonance down to the desired value of 199 MHz. Three or higher sets of arm cannot provide satisfactory S11 values, therefore, two sets of extra radiating arm have been selected as optimized design and prototyping testing. Fig. 7 (c) represents the effect of multiple sets of radiating arms.

B. Concrete Wall Climbing Robot Design

The wall climbing robot is designed to climb vertical reinforced concrete structures and carry the GPR as a payload. The robot's adhesion mechanism is based on rare earth neodymium magnets. The adhesion module's design incorporates a flux concentrator called 'yoke' that can concentrate and magnify magnetic flux towards reinforcement bars (rebars) to penetrate the concrete cover and achieve magnetic bonding. In order to achieve sufficient adhesion force to carry the GPR on a vertical plane, parametric studies of the adhesion module's design criteria such as the thickness of the yoke, effect of rebar mesh on adhesion and use of multiple yokes have been carried using Finite Element Analysis (FEA) software Comsol Multiphysics.

The adhesion module consists of three magnets arranged on the yoke as shown in Fig. 8. As the magnets are located in close proximity of each other, therefore, the distance between them, M_l will impact the resultant adhesion force. Simulation results show that the module can achieve 130 N of adhesion force at 30 mm concrete cover while 5×5×1 cm size of grade N35 magnets are used. The rebar diameter used is 12 mm and the results are shown in Fig. 9.

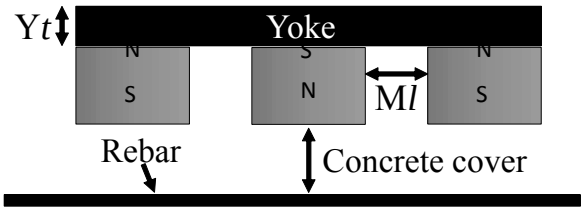

Fig. 8 Proposed structure of the adhesion module

Secondly, thickness of the yoke, Y_t is capable of concentrating magnetic flux lines towards rebars. Results suggest an increase in thickness can improve the adhesion significantly from 70 N to 102 N for 20 mm thick yoke. However, the adhesion force comes to a saturation point of approximately 85 N at 35 mm and more and further increases in thickness would not have any significant influence on the adhesion force. Moreover, the force-to-weight ratio, η starts to decrease due to added weight as shown in Fig. 10. A detailed study of the design parameter of the developed adhesion module can be found in [18].

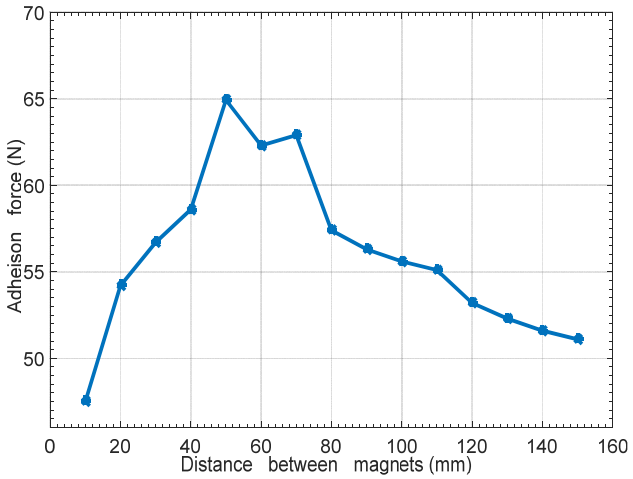

Fig. 9 Adhesion force at 30 mm air gap for different distances between the magnets, *Ml* [18]

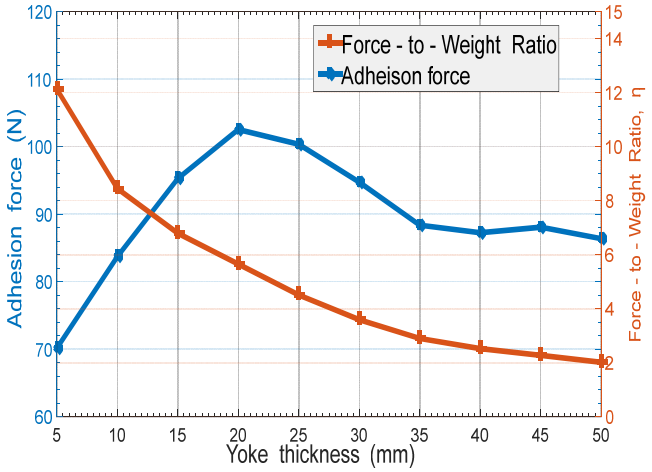

Fig. 10 Adhesion force and Force-to-Weight Ratio for different thicknesses of the yoke, *Yt* [18]

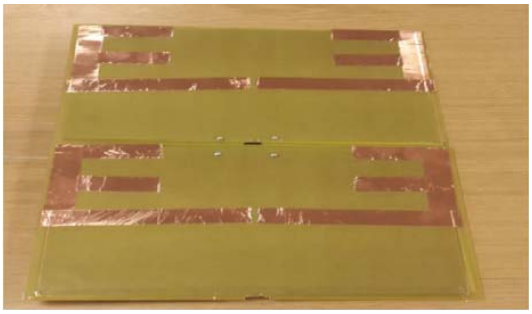

(a)

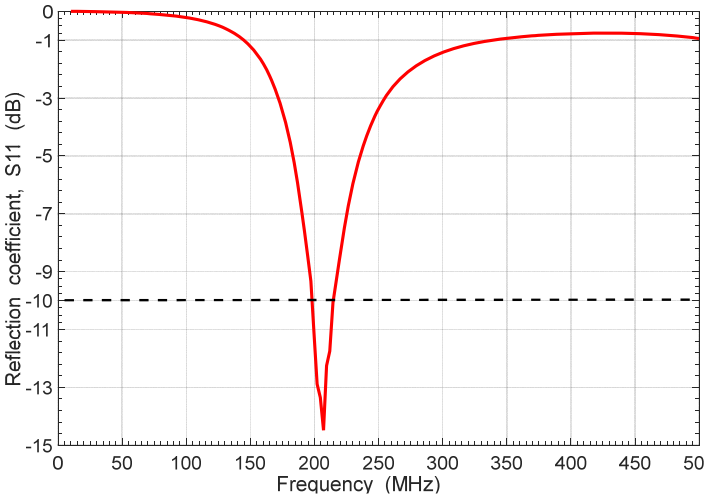

(b)

Fig. 11 (a) Top side of the fabricated miniaturized diploe antennas with extra radiating arms; (b) Measured S11 from the Agilent 4395Anetwork analyser

IV. System Integration and Measurements

To validate the simulation results and assemble the entire system, laboratory prototype of the proposed antenna and the climbing robot have been built.

A. Miniaturized Antenna Fabrication

A prototype antenna with two sets of additional radiating arm has been fabricated on a FR4 dielectric substrate (ε_r = 4.4). The antenna dimension is 40×20×0.2 cm. A 500 MHz Agilent 4395A network analyser is used for reflection coefficient, S11 measurement. Experiment result shows the antenna resonates at 206.1 MHz centre frequency with -14.8dB of S11. This is a +6 MHz of variation compared to simulations, however, the experiment results are acceptable and closely matched with simulations. The measured antenna has 14 MHz -10dB bandwidth and 1.9 dBi of directivity gain. The antenna fabricated with copper tape on a FR4 substrate and the reflection coefficient graph are given in Fig. 11.

B. Design of the Climbing Robot

The mobile climbing robot is built using a yoke dimension of 25×5×1.5 cm and same sized magnets as discussed in the simulation section. The outer dimension of the robot is 35×20×10 cm. The gap between the magnet surface and climbing surface is critical and the gap is kept to a minimum of 10 mm. A small gap increases the adhesion force significantly. The robot is equipped with two infra-red distance measurement sensors for vertical wall detection and two servo motors are used to fold and unfold the GPR antennas for the robot's floor-to -wall and wall-to-floor transition procedure. As a vertical wall is detected by the infra-red sensors while the robot is operating on the floor, the servo mechanism folds the antenna set backword for the front wheels to make contact with the wall. As the transition is completed and the robot is stabilized on the wall, the servo motor unfolds the antennas back to scanning position. The robot's net weight is 2.47 kg with on-board electronics and the antennas and can obtain maximum adhesion force of 110 N for 30 mm concrete cover. The measured adhesion force and the floor-to-wall transition procedure is shown in Figs. 12 and 13, respectively.

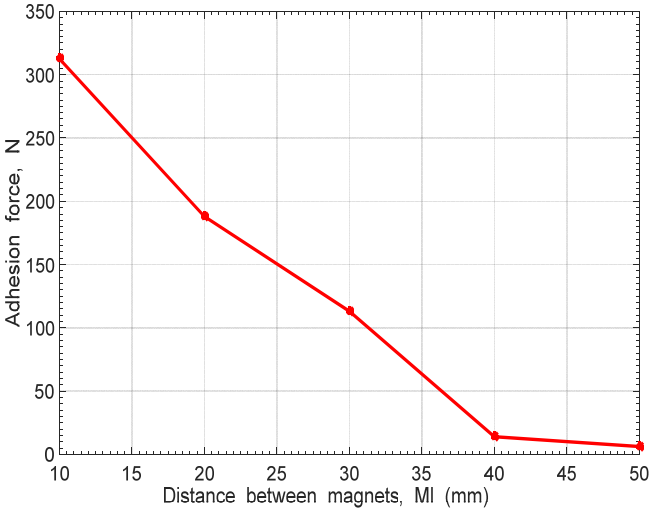

Fig. 12 Measured adhesion force [18]

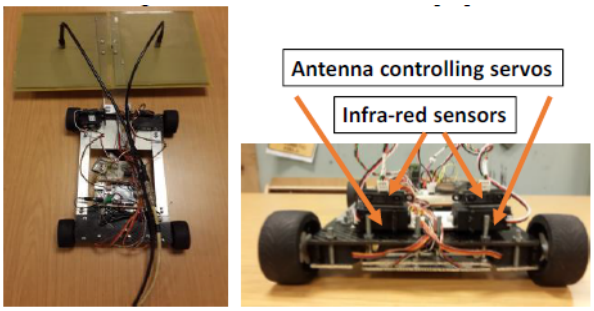

(a)

(b)

Fig. 13 (a) Top and front view (without the antenna) of the prototype robotic GPR system; (b) Floor-to-wall transition procedure

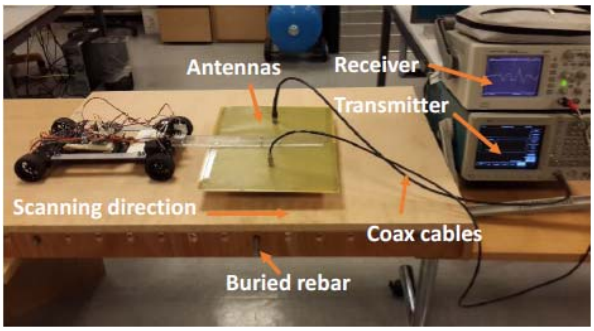

(a)

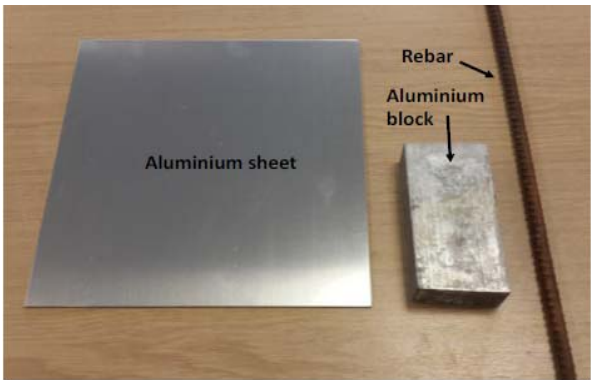

(b)

Fig. 14 (a) GPR measurement setup using the pulse generator and oscilloscope; (b) Target buried objects

C. Measurement Procedure and Results

Experiments are conducted to detect and localize buried objects. The application field of this proposed robotic GPR system is concrete structures inspection, therefore, to emulate the concrete inspection scenario, a test rig using wooden plate has been built. Concrete and wood have same dielectric constant of 1 and magnetic permeability of 1. So, a wooden plate can be used as a concrete cover. A 30 cm long and 1.5 mm thick aluminium plate, an aluminium block of 15×8×4 cm dimension and a rebar of 12 mm diameter have been chosen as target objects to be detected. The GPR transmitter consists of a pulse generator that generates a train of 5 ns full-width-half-maximum (FWHM) Gaussian pulse at -5 V peak-to-peak amplitude at 1 MHz repetition frequency. The GPR receiver consists of a 1 GSa/s sampling oscilloscope (Agilent DSO3102A) which visualizes the reflected signal captured by the receiving antenna. Fig. 14 presents the measurement setup and the target objects for the experiments. Each object has been placed under the wooden plate in turns and the GPR scanning is done separately for each object.

First, the reflected signals are captured for a 1.5 mm thick aluminium sheet. The robot is stopped and the reflected signal is captured at every 5 cm steps. A clear reflection from the aluminium sheet can be seen in profile 4 in Fig. 15 (a), where the GPR receiving antenna is located right above the sheet. The amplitude of the reflection starts to reduce as the robot travels away from the sheet. Likewise, to detect a block of aluminium for the size of, a scanning at 3 cm steps is carried out. Profile 3 of Fig. 15 (b) is found to be the position where the antenna is located right on top of the block. Same results have been found to detect a 12 mm diameter rebar located at 40 mm depth. In this case, profile 3 of Fig. 15 (c) shows the position of the antenna aligned right on top of the rebar. It shows a low amplitude signal because of the smaller size of the target, however, the peak of the reflection is clearly visible. Moreover, the time difference between the peak of the initial pulse and the reflected pulse is 3.2 ns. By using this two-way travel time, the measured distance is calculated to be 0.51 m. there is an error of 0.11 m between the actual and measured values. A higher resolution GPR with sharper pulse width can rectify this error. A low frequency GPR has a deeper penetration depth of up to 7 m according to the literature. However, a low amplitude pulse has been selected as the transmitting pulse in this work which reduces the penetration depth to about 50 mm.

V. Conclusions

In this paper, the design and testing of the concrete wall climbing robot for performing GPR surveys in vertical reinforced concrete structure have been presented. A low frequency 200 MHz GPR system has been designed using miniaturized antennas. The rationale of choosing a low frequency system is to keep the cost down and the keep the development process simple. The technique of implementing two sets of additional radiating arms has reduced the dipole antenna length by 40% compared to a conventional 200 MHz dipole antenna. This feature improves the portability of the system and provide a method for further miniaturization of high frequency system in the future. The assemble prototype robot exhibits good payload capacity and operational efficiency. Experiments demonstrate the capability of the developed GPR to detect and localize an aluminium sheet and a block, a rebar at up to 50 mm depth. Even though there was an error of 0.11 m, the implementation of narrower pulse of 1 ns or lower could improve the result and this is an aim for future work. The utilization of low amplitude transmitting pulses ensures the low penetrating capability which is suitable for concrete environment. The aim of this paper is to prove the concept and the deigned robot can be deployed to collect the radar data, allowing operators to safely perform grid or detailed surveys of potentially hazardous locations and

allowing them to process data offline from a safe location. Mobility testing confirms the robot's ability to perform floor-to-wall transition and vice-versa and radar testing confirms the viability of collecting radar data from a robotic platform.

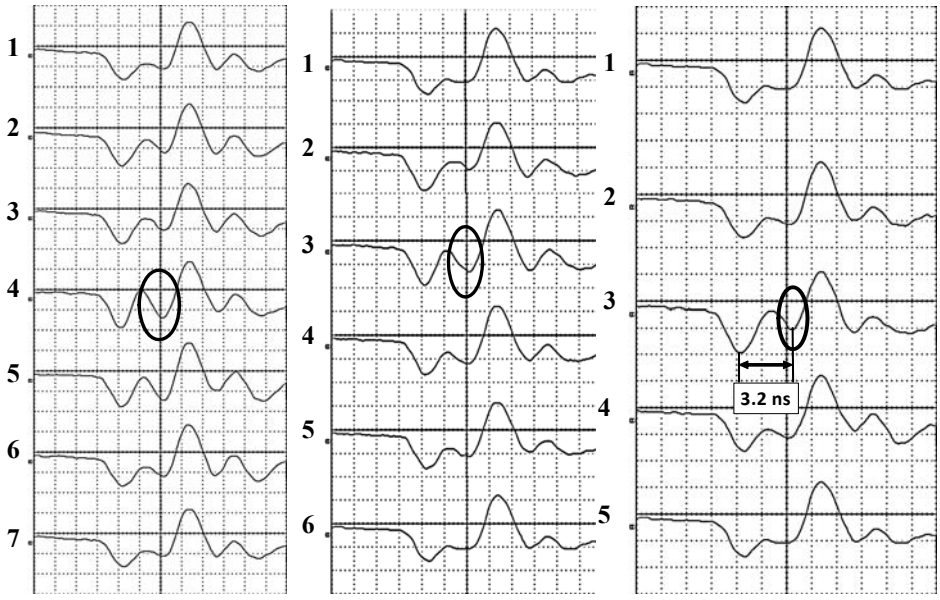

(a) (b) (c)

Fig. 15 Peak of the reflection from the target objects (shown in circle) for: (a) aluminium sheet; (b) aluminium block; (c) rebar.

Future work for this project is set to incorporate a high frequency system for robustness of the system as well as investigating resistive or capacitive antenna loading technique to increase the antenna bandwidth.

REFERENCES

[1] E. Pasolli, F. Melgani and M. Donelli, "Automatic Analysis of GPR Images: A Pattern-Recognition Approach," IEEE Transaction of Geoscience and Remote Sensing, vol. 47, no. 7, pp. 2206-2217, 2009.

[2] J. Francke, "Applications of GPR in Mineral Resource Evaluations," in International Ground Penetrating Radar Conference, Lecce, 2010.

[3] G. Grazzini, M. Pieraccini, F. Parrini, A. Spinetti, G. Macaluso, D. Dei and C. Atzeni, "An Ultra-Wideband High-Dynamic Range GPR for Detecting Buried People After Collapse of Building," in International Ground Penetrating Radar Conference, Lecce, 2010.

[4] E. Trautmann, L. Ray and J. Lever, "Development of an Autonomous Robot for Ground Penetrating Radar Surveys of Polar Ice," in IEEE/RSJ International Conference on Intelligent Robots and Systems, St. Louis, 2009.

[5] E. Utsi, "The Shrine of Edward the Confessor: A Study in Multi-Frequency GPR Investigation," in International Ground Penetrating Radar Conference, Lecce, 2010.

[6] D. Daniels, "Surface Penetrating Radar," The Institute of Electrical Engineers, London, 1997.

[7] T. Roackaway and J. A. Rivard, "Aplication of Ground Penetrating Radar in The Urban Environment," in International Ground Penetrating Radar Conference, Lecce, 2010.

[8] G. Borgioli, L. Capineri, P. Falorni, S. Matucci and C. G. Windsor, "The Detection of Buried Pipes from Time-Of-Flight Radar Data," IEEE Transactions of Geoscience and Remote Sensing, vol. 46, no. 8, pp. 2254-2266, 2008.

[9] G. Roqueta, L. Jofre and M. W. Feng, "Analysis of The Electromagnetic Signature of Reinforced Concrete Structures for Nondestructive Evaluation of Corrosion Damage," IEEE Transactions of Instrumentations and Measurements, vol. 61, no. 4, pp. 1090-1098, 2010.

[10] X. Dérobert, J. Iaquinta, G. Klysz and J. Balayssac, "Use of Capacitive and GPR Techniques for The Non-Destructive Evaluation of Concrete Cover," International Journal of NDT and E, vol. 41, no. 1, pp. 44-52, 2008.

[11] M. Howlader and T. Sattar, "FDTD Based Numerical Framework for Ground Penetrating Radar Simulation," Progress In Electromagnetics Research M, vol. 44, pp. 127-138, 2015.

[12] M. Yan, M. Tian, Lu Gan and X. Chen, "Impulse Ground Penetrating Radar Hardware System Design," in International Coference on ITS Telecommunications, Chengdu, 2006.

[13] M. Howlader and T. Sattar, "Finite Element Analysis Based Optimization of Magnetic Adhesion Module for Concrete Wall Climbing Robot," International Journal of Advanced Computer Science and Applications, vol. 6, no. 8, pp. 8-18, 2015.

[14] "IDS RIS Hi-Bright Ground Penetrating Radar for bridge condition assessment in Washington DC," The National Academies of Sciences, Engineering, and Medicine, Washington DC, 2013.

[15] C. Ekes and B. Neducza, "Robot Mounted GPR for Pipe Inspection," in International Conference on Ground Penetrating Radar (GPR), Shanghai, 2012.

[16] M. W. Rebecca, R. E. Laura, L. H. James and B. M. Amy, "Crevasse Detection in Ice Sheets Using Ground Penetrating Radar and Machine Learning," IEEE Journal of Selected Topics in Applied Earth Observations and Remote Sensing, vol. 7, no. 12, pp. 4836-4848, 2014.

[17] B. Zhiqiang, G. Yisheng, C. Shizhong, Z. Haifei and Z. Hong, "A Miniature Biped Wall-Climbing Robot for Inspection of Magnetic Metal Surfaces," in IEEE International Conference on Robotics and Biomimetics, Guangzhou, 2012.

[18] M. Howlader and T. Sattar, "Novel Adhesion Mechanism and Design Parameters for Concrete Wall-Climbing Robot," in SAI Intelligent Systems Conference, London, 2015.